Single- and multiple-electron dynamics in the strong-field tunneling limit

B. Sheehy, R. Lafon, M. Widmer, B. Walker,* and L. F. DiMauro
Chemistry Department, Brookhaven National Laboratory, Upton, New York 11973

P. A. Agostini
Service des Photons, Atomes et Molecules, Centre d'Etudes de Saclay, 91191 Gif Sur Yvette, France

K. C. Kulander
Theoretical Atomic and Molecular Physics Group, Lawrence Livermore National Laboratory, Livermore, California 94551
(Received 18 March 1998)

Evolution of atomic ionization into the strong-field limit offers the opportunity to study the fundamentals of atom-laser interaction. In this study, we report on high precision measurements of the ion and electron distributions from laser-excited helium and neon atoms which reflect the changing continuum dynamics as the ionization process evolves into the pure tunneling regime. The experiments present evidence of both single- and two-electron ionization. These data provide a direct quantitative test of various theories of strong-field ionization. We show that a relatively simple semiclassical model which includes a description of a field-driven electron elastically rescattering from an accurate ion core potential reproduces the measured electron distributions for both atoms. However, using this model to calculate e-$2e$ inelastic rescattering yields cross sections which are incompatible with the measured two-electron ionization. [S1050-2947(98)06111-3]

PACS number(s): 32.80.Rm, 31.90.+s, 32.80.Fb

I. INTRODUCTION

Over the past two decades, the study of the interaction of atoms with intense laser fields has resulted in a comprehensive understanding of the nonlinear physics and applied concepts relevant to short-wavelength generation and electron acceleration [1]. However, only recently has a comparable understanding of the underlying dynamics of the ionizing electron as it leaves the atom been achieved [2]. This advance was driven by significant progress in both experimental and theoretical capabilities. Experimentally, the advent of kHz repetition rate, high-peak-power lasers [3] has provided an essential tool necessary to span the entire intensity range of importance. At the same time, numerical solutions of the time-dependent Schrödinger equation have provided accurate and informative views of the excited electron dynamics [4]. The culmination of these is an intuitive model of strong-field rescattering [5,6] based on simple quasiclassical notions. Once an electron in a strong field has made the transition into the continuum from its initial bound state, its motion is dominated by its interaction with the external laser field. Approximately one-half of an optical cycle after the electron enters the continuum, the field can drive the electron back into the vicinity of the ion core, where it can undergo elastic or inelastic scattering, or be recaptured into the initial ground state by emitting a high-energy photon. The essential physics underlying the production of the observed high-energy photons and electrons is contained in these (re)collision events.

In 1964 Keldysh [7] showed that at infrared and visible wavelengths the dynamics of strong-field atomic ionization undergoes a change in character as the intensity increases. In weaker fields a bound electron will be promoted into the continuum by the simultaneous absorption of enough photons to increase its energy above its ionization potential. This is called multiphoton ionization (MPI). However, as the laser intensity increases, a completely different mode of escape becomes possible. At large distances from the nucleus the electrostatic attraction of the ion core can be overwhelmed by the laser's instantaneous electric field, producing a barrier through which the valence electron can tunnel. In this regime a quasistatic tunneling picture becomes appropriate: the laser field varies so slowly compared to the response time of the electron that the ionization rate becomes simply the cycle average of the instantaneous dc-tunneling rate. In the language of Keldysh, tunneling ionization (TI) becomes dominant when the ratio of the frequency of the applied field to the tunneling rate becomes less than unity. This ratio, known as the Keldysh or adiabaticity parameter γ, is given by $[I_p/(2U_p)]^{1/2}$, where I_p is the binding energy of the electron, and $U_p = 2\pi I/c\omega^2$ is the ponderomotive energy in atomic units of a free electron in a laser field of frequency ω and intensity I. The essential connection between the ideas of Keldysh and the rescattering picture lies in a deterministic view of ionization predicated by an electron tunneling into the continuum at a particular phase (amplitude) of the field.

The Keldysh theory prediction of the evolution to TI in strong fields has been confirmed by other, more rigorous, theoretical methods [8]. However, experimental access to the tunneling regime has been limited, hampering quantitative comparisons with the rescattering model. The reason for this is simply that for visible laser pulses, even as short as a 100 fs, ionization depletes the ground state (saturation) before the atom can experience intensities where $\gamma < 1$. Consequently, the majority of experimental studies on neutral atoms exposed to intense, short-pulse laser fields have been carried out in the MPI regime ($\gamma > 1$). The few experiments [9–12]

*Present address: Dept. of Chemistry, University of California, San Diego, LaJolla, CA 92093.

that have extended into the tunneling regime have been limited to observation of total ionization rates or electron energy distributions over a small dynamic range.

In this paper, we report on a systematic study of the strong-field ionization of helium and neon atoms in the tunneling regime. It has been shown [13,14] that because of their large binding energies, these two atoms tunnel ionize ($\gamma \sim 0.5$) near saturation with fs, titanium sapphire pulses. Thus, these atoms form a paradigm for our theoretical and experimental investigation of the subtle consequences produced by the rescattering of a tunneled wave packet with its parent ionic core.

First, the effects of elastic rescattering on the energy distribution of the electron are treated. Classically, an electron oscillating in an ac field can transfer part of this energy into a drift motion during the momentum exchange in an elastic recollision. While this possibility has long been recognized theoretically, the experimental verification was beyond technological capabilities. The reason for this is that the rescattered component does not exceed a fraction of a percent of the total ionization yield. Thus observation requires measurements over a more extended range of sensitivity. This capability became available only recently with the advent of kHz repetition rate, high-peak-power lasers [3]. In this work, the study of the electron energy and angular distributions and the total ionization rates over 12 orders of signal magnitude using intense, fs laser pulses at a kHz repetition rate provides the foundation for a quantitative testing of the rescattering model. A description of the experimental method is given in Sec. II A.

A relatively complete semiclassical rescattering model is developed in Sec. II B to mimic the time evolution of a tunnel-ionized, continuum wave packet in the *combined* fields of the laser and the ion core. This permits an effective means for analyzing the essential physics. The calculations incorporate realistic core potentials for both helium and neon. The objective is to achieve a description of the single- and multiple-electron dynamics as it pertains to the production of high-energy electrons, harmonic generation, and double ionization within the model's framework. We will show in Sec. III that inclusion of rescattering is essential, and yields calculated spectra which agree well with the observed electron energy and angular distributions.

A second central issue to this paper, discussed in Sec. IV, involves the nature of strong-field multielectron ionization. This long-standing, unresolved problem predates most of our current physical understanding of strong-field single-electron dynamics, and a brief account of the history may be found in a recent review [2]. We present accurate measurements of the total yield for singly and doubly ionized helium and neon at different wavelengths. These data establish that in a linearly polarized field the rate for two-electron ejection is orders of magnitude larger than that which would be expected if the ionization proceeded sequentially—single ionization of the neutral first, followed by single ionization of the ion. Our rescattering model when applied to an e-$2e$ inelastic process fails, both quantitatively and qualitatively, to reproduce the measured nonsequential yields of doubly charged helium and neon atoms. Section V contains a discussion of the applicability of the rescattering model for describing single- and two-electron dynamics in a strong laser field.

II. METHOD

A. Experiment

In the experiments presented here a 120-fs, 1-kHz repetition rate, titanium sapphire laser operating at 0.78 μm was focused by $f/4$ or $f/6$ optics into an ultrahigh-vacuum chamber. Under these conditions, the system is capable of producing a maximum intensity of 20 PW/cm^2 with typical pulse-to-pulse fluctuations $<1.5\%$ for 10^6 laser shots. The studies at 0.39 μm were performed by frequency doubling the output in a 0.7-mm-thick BBO crystal. At this wavelength a maximum intensity of 2.5 PW/cm^2 is obtained using $f/4$ optics. The laser polarization is $>99\%$ over the entire intensity range. The laser intensity is calibrated by measuring the short-pulse resonant photoelectron spectrum of xenon as a function of pulse energy, and recording, during each data run, the xenon and helium or neon total ion yields. The calibration is corroborated by a spot size measurement and accurate to approximately 25%. The helium and neon samples were high-purity 99.999% gases which were further in-line scrubbed to <0.1 ppm for O_2, H_2, H_2O, CO_2, and hydrocarbon impurities. A 30-cm-long time-of-flight photoelectron spectrometer (PES) provides energy and angular resolution of 0.05 eV and 65 mrad, respectively. The spectrometer's energy calibration was obtained by recording the long-pulse, high-order (>40 photon absorption) above-threshold ionization (ATI) spectrum of xenon. A 30-cm time-of-flight mass spectrometer provides sufficient resolution ($m/\delta m > 300$) to easily separate H_2^+ and He^{2+} mass peaks. The e/m detection sensitivity for the singly and doubly charged ions is determined from analyzing the ion yields at the saturation intensity. This eliminates any uncertainty in the microchannel plate response and detection electronic bias. Data collection used 1-ns binning of discriminated electron and ion events operating at a low event probability ($\leqslant 0.25$/shot), ensuring space-charge-free conditions. For the collection of the ion yield and ratio data a veto signal derived from the laser-pulse energy is applied to reject pulse variations outside of a predefined energy window. Depending upon the study the window is varied between $\pm 1\%$ and 5%. To ensure accuracy in the measure of the ratio of double-to-single ionization (σ^{++}/σ^{+}), the ions are concurrently collected at a fixed intensity and averaged for at least 10^6 laser shots. The current photoelectron spectra were recorded between 0.5 and 1.5 times the saturation intensity ($I_{\mathrm{sat}}^{\mathrm{He}} = 0.8$ PW/cm^2 and $I_{\mathrm{sat}}^{\mathrm{Ne}} = 0.6$ PW/cm^2) for neutral helium and neon, respectively. Angle-resolved PES (ARPES) were recorded at these intensities, and the total distribution constructed by integration over the polar angle and assuming azimuthal symmetry around the polarization axis. Walker *et al.* [13] showed that contributions due to sequential ionization of He^+ remain insignificant up to an intensity of ~ 4 PW/cm^2, while the current study shows a similar behavior for neon.

B. Theory: Quasiclassical rescattering model

The demarcation between the ionization pathways, multiphoton versus tunneling, becomes apparent when the wave packets promoted from the bound state into the continuum in these two limiting cases are considered. In the MPI regime, an ionized population appears continuously, at all phases of

the field. To conserve momentum, this transition must take place while the electron is close to the nucleus, producing a continuum wave packet initially localized near the ion core. When the intensity increases to the point that $\gamma<1$, TI begins to dominate, and the electron is released a significant distance from the nucleus. During a narrow time interval near the maximum in the oscillating electric field, an asymmetric, delocalized wave packet emerges at the outer edge of the suppressed Coulomb barrier. The overall symmetry of the ionization process is maintained by a complementary wave packet being generated on the opposite side of the nucleus one-half cycle later. Clearly, the evolution of the continuum wave packets in these two limiting cases can be very different, and is reflected in our experimental results.

Generally in the MPI regime, the amplitude of oscillation of a free electron for optical laser frequencies is not significantly larger than the effective range of the atomic potential, which we define to be the point where the electric field of the laser exceeds the Coulomb attraction of the ion core. In this case the excited wave packet continues to interact with its parent ion core until it gains sufficient energy to escape completely. Because this excitation is near the nucleus, the MPI wave packet can include Rydberg-state components, leading to resonant enhancement of the ionization and its corresponding signature of narrow-peaked substructure in the ATI spectrum. On the other hand, the motion of the continuum wave packet in the tunneling limit is controlled mostly by its interaction with the laser field, since it rapidly moves beyond the effective range of the ion core potential. Its evolution can be reasonably represented using the classical equations of motion for a laser-driven electron. In a simple quasiclassical (SQC) model for TI [9], the bound electron tunnels free at a particular phase ωt_o of the field, then undergoes oscillatory motion at the laser frequency, ω. The electron-field interaction in the length gauge can be written as $e\varepsilon\hat{z}\sin\omega t$, where $\hat{z}$ is the direction of polarization and $\varepsilon=(8\pi I/c)^{1/2}$ is the slowly varying amplitude of the laser's electric field. Assuming that the electron is initially at rest after tunneling, its velocity is given, in atomic units, by $v(t)=(\varepsilon/\omega)(\cos\omega t-\cos\omega t_o)$, where the first term represents the field-induced quiver motion, and the second term the drift velocity which is established the instant the electron appears in the continuum. In a short-pulse experiment, the detected photoelectron energy is determined by the drift velocity; the quiver energy is returned to the field as the intensity declines. Therefore, in the absence of further interactions with the ion core (rescattering) the maximum drift energy an electron can have is easily shown to be $2U_p$.

The rescattering picture [5,6] goes beyond the SQC model by recognizing that although in the tunneling regime electrons released into the field are initially accelerated away from the ion core, roughly half the electrons are driven back across the plane of the nucleus when the direction of the laser electric field has changed sign. During the time interval between when the electron tunnels free and its return to the ion core, the TI wave packet propagates for at least half an optical cycle beyond the effective range of the ion core potential, spreading freely in the transverse directions. Analysis of classical trajectories for the ionized electrons shows [6,14–16] that photoelectrons with energies $>2U_p$ are produced by trajectories which experience very large deflections (elastic backscattering, $\theta>\pi/2$) when they rescatter from the ion core. The final drift energy is determined by the phase of the optical field at recollision and the electron's scattering angle [17]. The elastic differential cross section in the backward direction can be approximated by that for Rutherford (Coulomb) scattering, $[\sigma(\theta)\sim(1/E^2)\csc^4(\theta/2)]$ [18], which varies slowly over the critical angular range producing the flat energy distribution for these PE's. The hard collisions (small impact parameters) necessary for producing large changes in drift energy also result in broader angular distributions for these high-energy electrons.

We have extended the SQC model to include the effects of the *first* re-encounter of the tunneling wave packet with the ion core. Subsequent collisions are ignored since the transverse expansion of the wave packet makes them substantially less effective. The rescattering model calculations proceed as follows: We divide the optical cycle into a large number (1600 points) of equal-time intervals. In each interval a trajectory is launched at the outer turning point of the suppressed effective potential with zero velocity. We follow the trajectory of the electron in the combined fields of the laser and the helium (neon) ion core until it either escapes or returns to cross the plane perpendicular to the field polarization at the nucleus. Those which escape contribute to the spectrum below $2U_p$ according to their drift velocities as in the SQC model. The returning trajectories are assumed to be guiding a freely spreading Gaussian wave packet whose width is given by $\alpha(\tau)=(\alpha(0)^2+[2\tau/\alpha(0)]^2)^{1/2}$, where $\alpha(0)$ is the initial width and τ is the propagation time between tunneling and return. Choosing $\alpha(0)=4.0a_0$ gives a return width consistent with our fully quantum-mechanical numerical studies [13]. A similar value for the initial width is found using an exact analytic solution derived for scanning tunneling microscopy [19] and applied to the problem of strong-field above-threshold ionization in a zero-range potential [20]. We calculate the differential elastic scattering cross section for this wave packet using [18]

$$\sigma(\theta)=\left|\frac{1}{2ik}\sum_{l=1}^{l_{\max}}a_l(2l+1)e^{2i(\eta_l+\delta_l)}P_l(\cos\theta)\right|^2, \quad (2.1)$$

where δ_l is the Coulomb phase shift (for a charge of 1), and η_l is the additional phase shift resulting from the short range part of the He^+ (Ne^+) potential. These phase shifts are obtained from numerical integration of the scattering equations for electron-He^+ (Ne^+) over the necessary range of energies and angular momenta. The partial-wave amplitudes, a_l are determined from the distribution of the impact parameter, b, in the returning wave packet ($l=mv_{\rm ret}b$).

Equation (1) gives the field-free differential cross section. The laser field will distort this nascent angular distribution. The transverse component of the outgoing velocity is conserved, but the velocity along the polarization direction has both a drift component and a quiver velocity which depend on the phase of the laser field at the return time. Drift velocities corresponding to PE energies as high as $10U_p$ can be produced if the electron is scattered by $\sim$180°. The total angle-resolved electron distribution for a given laser intensity is obtained by summing the contributions from all time intervals. The energy and angular distributions for the wave packet in each time interval are weighted by the instanta-

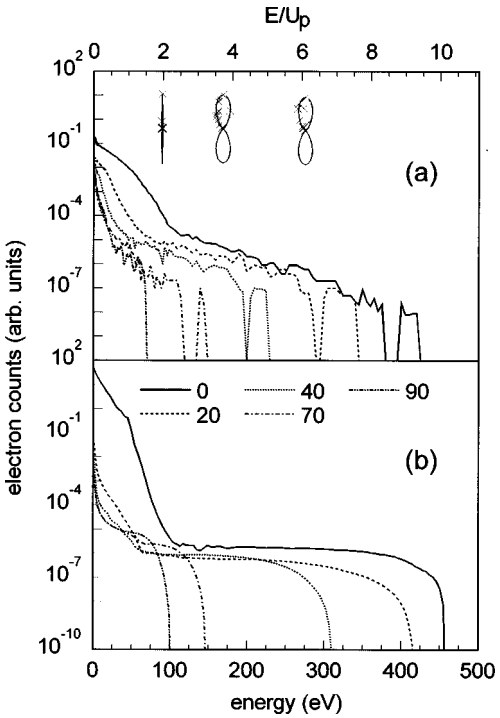

FIG. 1. The (a) measured and (b) calculated helium ARPES for five different emission angles at a saturation intensity of 0.8 PW/cm^2 and a wavelength of 0.78 μm. The abscissa is presented in absolute and scaled energy units. The polar plots in (a) show the measured angular distributions (crosses) at the indicated energies, and the solid lines are only to guide the reader.

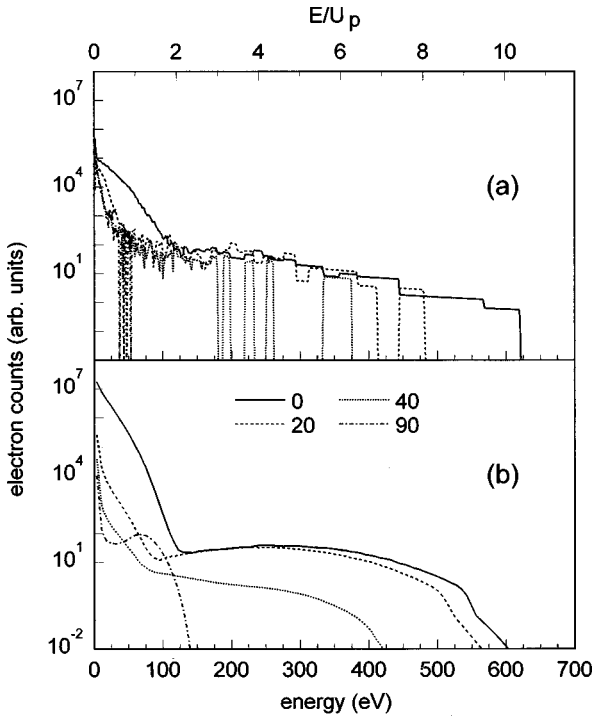

FIG. 2. Measured neon ARPES for four different emission angles at an intensity of 1 PW/cm^2.

neous tunneling rate when it was initiated. In these calculations we have actually used a scaled dc-tunneling rate which, when cycle averaged, gives the ac tunneling or Ammosov-Delone-Krainov (ADK) rate [21]. This accounts for the initial state not being purely hydrogenic. Spatial and temporal averaging are performed for comparison to the experimental measurements. To further facilitate comparison, the calculated angle-resolved PES are reduced to minic the experimental acceptance angle of the spectrometer. The magnitude of the nonsequential, double ionization yields due to rescattering is calculated at the same time using an effective total inelastic cross section which accounts for both excitation (which lowers the energy threshold) and ionization. In these strong fields, any excited state of the ion will be ionized during the next few cycles, and therefore are counted as yielding the double ion.

III. SINGLE-ELECTRON IONIZATION

Tunneling photoelectron distributions

Figures 1(a) and 2(a) show the experimental ARPES near the saturation intensities for helium and neon, respectively. The abscissa is presented in absolute and scaled (E/U_p) energy units and $\gamma \simeq 0.5$ for both figures. The ponderomotive energy associated with the peak intensity is used to define the scaled energy. The ARPES are recorded through a 65-mrad solid angle while rotating the laser polarization relative to the spectrometer's axis. The spectra extend to extremely high energy, and are structureless when compared to the photon energy, i.e., no resonant or ATI peaks are discernible. At lower intensity where MP ionization dominates, broad ATI structures are visible in the spectra from both atoms [13]. The phenomenological disappearance of ATI structure is a consequence of the experimental averaging, and is observed at $\gamma \sim 0.75$ or one-half the saturation intensity. In the TI regime, the increase in the ionization rate with intensity is much slower than in the MP regime, so that the observed photoelectrons are produced from a relatively broad range of intensities. Since the ac Stark shift of the continuum is much larger than the photon energy and is position dependent, the spatial averaging washes out any structure in the measured energy distributions even though our single-atom calculations show the ATI structure persists well into the tunneling regime. An experimental spectrum which somehow was confined to a single-peak intensity would show the ATI structure even in the TI regime.

The ARPES in Figs. 1 and 2 seem to be a superposition of two components: a ''normal'' narrow distribution that falls off rapidly with increasing energy between 0 and $2U_p$, and a much broader but weaker, almost flat energy distribution that extends out to $(8-10)U_p$, as expected from classical backscattering. The striking difference in angular anisotropy for the two components is apparent in the polar plots of Fig. 1(a). This behavior differs dramatically from all previous experimental reports [2]. For example, the photoelectron distributions for inert gas atoms [22,15] clearly show angle-dependent structures, as well as an abundance of electrons with energies $>2U_p$. We believe these differences reflect the pure tunneling nature of these results, and therefore provide a unique opportunity for quantitatively testing the rescattering picture.

Total PE distributions are shown in Figs. 3 and 4 for helium and neon in both absolute and scaled energy units. The distributions are constructed by integrating the experimental ARPES over the polar angle and assuming azimuthal

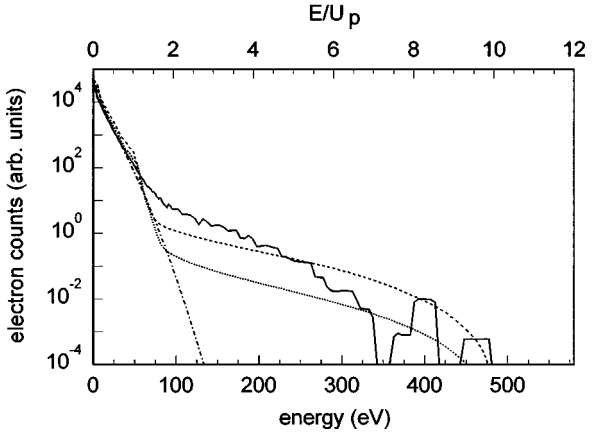

FIG. 3. Total helium photoelectron energy distribution for 0.78-μm excitation at 0.8 PW/cm^2. The measured distribution (solid line) is compared to calculated distributions using the semiclassical model. The dashed and dotted lines incorporate rescattering from a He^+ and pure Coulomb potential, respectively. The calculated PES without rescattering is given by the dash-dotted line. The calculated curves include both spatial and temporal averaging for direct comparison to the experiment.

symmetry around the polarization axis. Figure 3 shows the helium distribution at 0.8 PW/cm^2, and Fig. 4 plots the helium (solid circles) and neon (open circles) distributions at 1.0 PW/cm^2. The figures show that, in absolute units, an increasing laser intensity results in the production of higher-energy electrons, but in energy units scaled to U_p, the PE distributions for both intensities and atoms are similar in shape. This illustrates an important fundamental principle that the scaled classical dynamics of a tunneled electron is intensity invariant.

Inspection of the spectra shown in Figs. 1–4 show a qualitative behavior consistent with the classical picture of TI discussed above. In fact, the distribution of the majority of photoelectrons is predicted quite accurately by the SQC model: their energies lie below $2U_p$ and, up to this limit, are strongly aligned along the laser polarization direction (see the polar inset in Fig. 1). However, the striking transition that

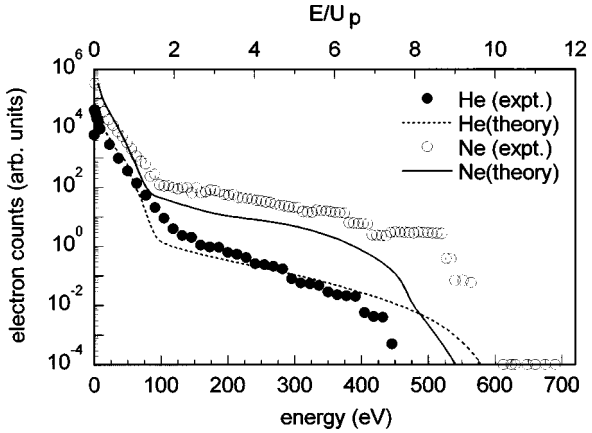

FIG. 4. The measured total photoelectron energy distribution for helium (solid circles) and neon (open circles) for 0.78-μm excitation at 1 PW/cm^2. The averaged calculated curves for helium (dashed) and neon (solid) incorporates rescattering from realistic He^+ and Ne^+ potentials, respectively.

occurs above $2U_p$ clearly indicates that representing the complete ionization dynamics requires a more sophisticated model. As discussed above, we expect that rescattered electrons will have a relatively broad, flat angular distribution with a gradual fall-off with energy up to $\sim 10U_p$, the maximum energy observed. We emphasize that the scaling with U_p of the spectral characteristics establishes that it is the dynamics in the continuum that is most important. There is a distinct correlation between the scattering direction and the cutoff in the energy distribution [15,17]. This is simply understood by considering the trajectories of elastically scattering electrons. The huge change in the drift energy of rescattered electrons is due to acceleration by the field. As mentioned earlier, the field can affect only the velocity component along the polarization direction. This means it is potentially most effective for backscattered electrons (the 0° on-axis spectra of Figs. 1 and 2), and less so as the scattering angle increases (off-axis spectra), leading to the observed connection between the direction and maximum energy.

Qualitatively, the PES in Figs. 3 and 4 provide some immediate insight into the significance of the spreading of the TI wave packet and the elastic scattering cross sections. The number of high-energy electrons is small because the transverse expansion of the TI wave packet causes most returning trajectories to have very large impact parameters. Our earlier numerical studies on neutral helium using the single-active-electron (SAE) approximation [4] found that the returning wave packet at this wavelength has a radius of approximately $30a_0$ as it rescatters from the nucleus [13]. In neon the width is found to be similar in magnitude. For a given atom this return width does not depend on the laser intensity but only on the free propagation time, and therefore only on the laser wavelength. Furthermore, Fig. 4 shows that at the same intensity where the excitation rates for both atoms are approximately the same, neon yields a factor of 10 more electrons beyond $2U_p$ than helium. This observation is compatible with the larger neon ion core having a larger elastic scattering cross section. The result is consistent with the more than an order of magnitude decrease in conversion efficiency observed between helium and neon for high harmonic generation [23] (HHG). Note that the measured energy distribution for neon extends further in energy than for helium partly due to the better counting statistics.

Quantitative comparisons between the measured and calculated total (spatial and temporal averaged) PE spectra are included in Figs. 3 and 4 for helium and neon, respectively. In Fig. 3 three different degrees of approximation in our calculations are shown. The dash-dotted line is calculated using the SQC model. As expected above the high-energy portion of the spectrum is absent. The SQC curve does not cut off abruptly at $2U_p$, since we allow our initial tunneling wave packets to have a finite longitudinal spread along the polarization direction. If the experiment did not have the dynamic range to include the high-energy tail (see Ref. [12], for example), one could conclude that the complete physics is contained in the SQC model, or other models which ignore rescattering [24]. The dotted and dashed curves are calculated incorporating the effects of elastic rescattering for a single, initial return of the wave packet. The dotted curve assumes a pure Coulomb interaction, and the dashed curve is calculated using a realistic e^--He^+ potential. The latter is

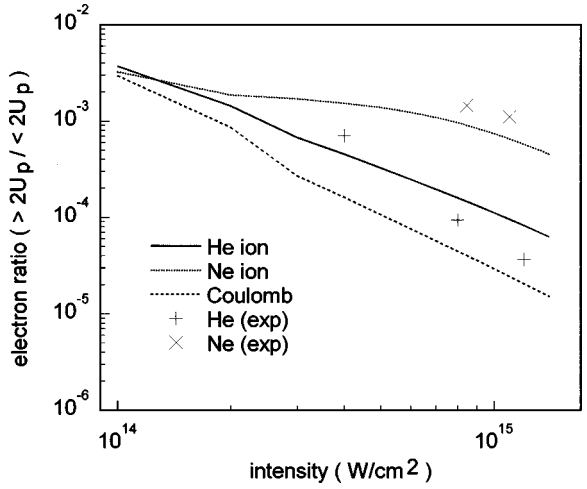

FIG. 5. Compiled helium and neon experimental (symbols) and calculated (lines) ratio of the total number of electrons with energies $>2U_p$ over those $<2U_p$ as a function of intensity for 0.78-μm excitation. The curves for the averaged calculated ratio are for Coulomb (dashed), He^+ (solid), and Ne^+ (dotted) rescattering.

more attractive at short range due to the less complete screening of the doubly charged nucleus. The use of the helium ion potential results in excellent agreement with the experimental measurement over the entire energy range, while the pure Coulomb scattering result underestimates the high-energy plateau. Equally good agreement between experiment (solid circles) and theory (dashed line) for helium is shown in Fig. 4 at a higher intensity (1 PW/cm^2). Figure 4 further demonstrates that the rate at which the ''hard'' backscattering collisions produce high-energy electrons is strongly affected by the exact nature of the short-range part of the potential. The measured enhancement for producing high-energy electrons in neon (open circles) relative to helium is well duplicated by our calculation (solid line) using a realistic SAE e^--Ne^+ potential.

Our measured results for helium and neon at different intensities are summarized in Fig. 5 along with calculated curves. We plot the ratio of the number of electrons with energies $>2U_p$ to those with energies $<2U_p$ as a function of intensity. The open and filled circles are the ratios derived from the measured total PES for helium and neon, respectively. The three calculated curves are the ratios obtained from the spatially and temporally averaged results using either the pure Coulomb (dashed), the He^+ (solid), or Ne^+ (dotted) potential. The measured helium ratio agrees well with the calculated curve (solid line) for the two highest intensities, but differs for the lowest intensity due to the multiphoton contributions which are not included in these calculations. This is consistent with our earlier work [13] which concluded that the transition to MPI occurs below 0.6 PW/cm^2. The curve calculated using the Ne^+ potential also shows good agreement with the measured ratios. In fact, the calculation verifies the larger ratio for neon compared to helium for the two highest intensities. The curve for the Coulomb case underestimates the ratio at higher intensities, although all three curves converge as the intensity decreases. This is because at the highest intensities used in the current study, the TI wave packet, which has a maximum instantaneous return kinetic energy of $3.2U_p$, produces collisions with energies in excess of 150 eV. Thus it is not unexpected that such hard collisions effectively penetrate the core, sampling the short-range part of the potential. This condition is relaxed at lower intensity because the reduction in the electron's return energy results in ''softer,'' less penetrating collisions. Of course, experimental access to this regime becomes impossible due to the evolution of the ionization dynamics into MPI ($\gamma>1$).

Our calculations also provide angle-resolved PES, as shown in Figs. 1(b) and 2(b). Although they are much smoother than the measured values, they reproduce the angle-dependent energy cutoffs and the flatness of the high-energy component. This agreement exists for all other intensities studied except at the highest intensity. In this case the measured PE spectrum ends around 10–20 % lower energy than we predict. This can be attributed to the poorer statistics in the measurement for the most energetic electrons at the highest intensity.

We have considered only the first return of the wave packet, and neglected coherent terms in evaluating the differential cross sections. Although these effects may alter the calculated values, the agreement we obtain indicates that the discrepancies are unlikely to be larger than factors of 2–4. It has been proposed [25] that the Coulomb field of the ion core can refocus the returning wave packet, making close collisions on the second or higher returns even more effective than the first. We believe our results provide evidence that this effect cannot be as large as was predicted. We will discuss this further in Sec. IV.

IV. DOUBLE IONIZATION AND THE RESCATTERING MODEL

Many-body effects form the basis of problems which are fundamental and central to our understanding of atomic physics. Well-documented investigations of single-photon double ionization of helium and other inert gases have provided a wealth of information about the role of electron correlations [26]. However, the nature of two (multiple) electron ejection in an intense laser field remains largely unresolved, despite the careful efforts of many groups [2]. The difficulty lies in the interpretation of the experiments which are not strictly unambiguous, as is the case for single-photon ionization. The same dynamics of an intense fs pulse, interacting with an atom responsible for determining the ionization regime, often leads to stepwise or sequential ionization of multielectron atoms [27]. In this scenario, ionization to higher charge states proceeds by a series of one-electron ejections from the ionic ground state, and can therefore be treated within a single-electron approximation. In this section, we will concentrate on the special case where the double (or nonsequential) ionization probability is orders on magnitude larger than the corresponding sequential process. Furthermore, ionization in the tunneling regime reduces some of the ambiguity present in the MP regime [28,29].

Beginning around 1983 [30], there have been a series of measurements on helium which showed clear evidence of enhanced double ionization above 10^{14} W/cm^2. Helium double ionization requires a minimum of 51 Ti:sapphire photons at 0.8 μm. The fraction of ''nonsequential'' ionization is observed to be $He^{+2}/He^+ \sim 1/400$ [13,31] at saturation.

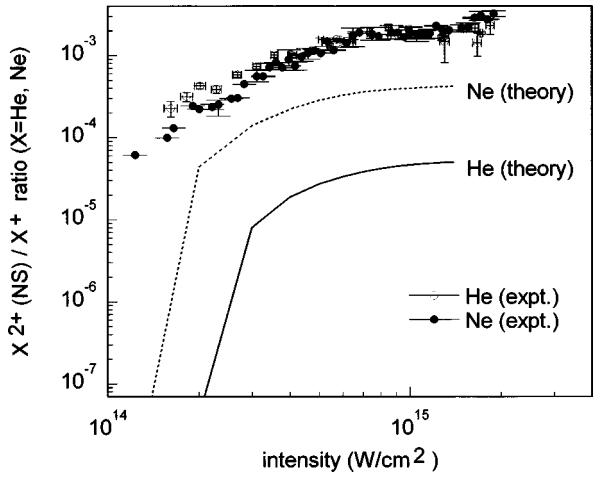

FIG. 6. Compiled experimental (symbols) and calculated (lines) ratio of nonsequential double-to-single ionization for helium and neon at 0.78 μm. The uncertainty for the measured ratio for helium and neon are given by the error bars. The helium and neon calculated curves are given by the solid and dashed lines, respectively.

This surprisingly efficient double ejection is unlikely to be attributable to resonance effects because the helium doubly excited states are well above the first ionization threshold, by over 35 eV, so that they cannot be expected to be strongly excited by the optical field. Similar results are observed for neon [32], where again the doubly excited states are far above the first ionization threshold. In fact, there have recently been reports of what appears to be direct triple ionization in rare gases [33]. The precise mechanism for simultaneous multielectron ejection in the absence of resonant intermediates is a subject of considerable debate at this time. Unfortunately it is beyond the present capabilities of any rigorous theoretical approach to treat two electron excitation and ionization for these wavelengths and intensities. However, recently a number of approximate models have attempted to address this problem. We will discuss this work more completely below, and present an analysis of the experiment using our quasiclassical rescattering model.

In addition to the photoelectron measurements presented in Sec. III, total ion yields as a functions of intensity were collected for both helium and neon. Walker *et al.* [13] demonstrated the versatility of kHz laser systems for increasing the sensitivity of total ion yield measurements. In fact, the dynamic range of this study of the helium ion yields surpassed previous reports by five orders of magnitude. This data not only provide an accurate test of calculated rates but also offer some revealing insights into the physics of strong-field double or nonsequential (NS) ionization. For instance, the NS production of He^{2+} was shown to be linked to the tunneling dynamics of the first electron, even when MPI dominates.

A sensitive measure of the nonsequential dynamics is provided by plotting the intensity dependence of the X^{2+}/X^{+} ratio (X=He or Ne) for both helium (open circles) and neon (solid circles) for 0.78-μm excitation, as shown in Fig. 6. To ensure accuracy, the two charge states are concurrently collected at a fixed intensity and averaged for at least 10^6 laser shots. The plot shows that the measured NS yield is similar for both atoms, achieving a value of 0.0020 [3] for helium and 0.0018[4] for neon at their respective saturation intensities. Below saturation, the ratio of each decreases by approximately a factor of 10 over the measured intensity range, although the absolute rates are changing by seven orders of magnitude. Furthermore, analysis [14] shows that both the NS helium and neon yields scale with the TI rates, calculated using ADK. We believe this provides an important clue to the NS mechanism; whatever the escape dynamics of the second (inner) electron, the first electron must tunnel into the continuum.

A number of attempts have been made to explain the dynamics of this surprisingly strong NS ionization. Fittinghoff *et al.* [31] proposed that correlation between the atomic electrons would cause a second electron to be either excited or ionized as the first electron tunnels free. In this case, the excitation of both electrons would be prompt and involve some degree of ground- or excited-state correlation. To test this ''shake-off'' mechanism would require a calculation of the dynamics of two electrons in an intense, pulsed, optical frequency laser field. This appears to be well beyond current computational capabilities, so a rigorous test of this mechanism has not been accomplished.

An alternative NS ionization mechanism is based on the rescattering model that we have shown can successfully characterize photoelectron distributions. It was proposed [6] that when the TI wave packet recollides with the ion core the second electron is promoted into the continuum via an e-$2e$ collision process. This unquestionably will occur, but calculations that have tried to estimate the significance of this mechanism have given mixed results [6,13,25,32]. Several independent experiments, both in helium [31,34,35] and neon [32], give values for the double-to-single ionization ratio at saturation consistent with the present work. General inspection of the experiment raises several issues which must be considered. First, the NS ionization in Fig. 6 is observed to have no intensity threshold. Returning electrons are known to have a maximum classical kinetic energy of $\sim 3.2U_p$ assuming zero initial energy which is independently verified by the high-energy cutoff in high-order harmonic spectra [5,23]. Therefore, we can determine a minimum intensity required for the rescattering electron to have enough energy to excite a core electron. In both He and Ne, NS ionization is observed to occur at intensities well below the expected thresholds. Second, the NS rate is found to have a much stronger dependence on the ellipticity of the laser field than the sequential processes [28,32,34,35], and is essentially extinguished with circularly polarized light. The rescattering model can explain this decrease in the NS yield as the polarization departs from linear, because the field will guide the returning wave packet away from the ion core if the ellipticity is too large. In fact, Dietrich *et al.* [32] showed a connection between the polarization dependence for both the NS and harmonic rate in neon using a rescattering approach. Finally, we must explain the observed magnitudes of the NS fraction. As we show below, the width of the wave packet at the first return is so much larger than the effective inelastic collision cross section, that the resulting e-$2e$ ionization probability is much smaller than the measured NS value.

The complete quasiclassical calculation, introduced in Sec. II B, can be used to predict the double-to-single ionization ratio produced from e-$2e$ inelastic rescattering. First we

must make clear what the assumptions of this rescattering mechanism for NS ionization are. In the first step, an electron tunnels free while at the same time the remaining electron(s) must relax into the ground state of the ion core. If the tunneling step is at all nonadiabatic, that is, if the ion is not left in its ground state, we should consider this to be a ''correlated'' pathway to double ionization. At the intensities under consideration, all excited states of the ion can be rapidly ionized by the field alone without any further interaction with the TI wave packet. Thus we would have either simultaneous double ionization if the nonadiabaticity promotes the second electron directly into the continuum, or resonance-enhanced sequential ionization if the second electron is ''shaken up'' temporarily into an excited state. We note that ion yield experiments alone cannot distinguish between any of these mechanisms. Therefore to evaluate the *rescattering* NS ionization yield accurately, it must be assumed that the first step is completely adiabatic. The second step in this mechanism is when the ionic ground state, which by itself is essentially unaffected by the laser field because of its much larger binding energy, is excited by the rescattering electron, at least into an excited state, eventually yielding a double ion. The operative threshold, then, for this energy transfer is on the order of the field-free excitation energy of the lowest excited state of the ion: ~40 and 27 eV for helium and neon, respectively. Using the semiclassical rescattering model described above, it is straightforward to perform a test of this NS ionization mechanism.

We express the effective inelastic cross-section using a modified e-$2e$ Lotz-type formula [36]. The cross section used is the sum of the field-free excitation and ionization cross sections for the ion. It has been shown [37] that the use of field-free cross sections is a reasonable approximation since the slowly varying (on the time scale of the collision) electric field from the laser has a very small effect on the inelastic scattering processes. In fact it was found that the field could either enhance or inhibit the excitation of the ion, but the effect was at most on the order of 10–20 %. For each trajectory we determine the probability for excitation by comparing the returning wave packet width to the inelastic cross section at the appropriate collision energy. In Fig. 6 we show the spatially and temporally averaged results for both helium (solid line) and neon (dashed line). Clearly, the e-$2e$ rescattering mechanism severely underestimates the absolute measured ratio, as well as differing substantially in its intensity dependence. The ratio of the experimental to calculated values at saturation are 47 for helium and 5 for neon. This means rescattering may play a role in neon NS ionization near the saturation intensity, but it is not the dominant effect even there. Furthermore, at lower intensities, the difference becomes enormous as the return energy falls below the minimum required for excitation. We believe this lack of agreement is a clear indication that more than inelastic rescattering is involved in the physics of NS ionization. Additionally, considering the order-of-magnitude difference in the e-$2e$ cross sections, it is difficult to rationalize in a rescattering picture why the double-ionization ratios would be the same for helium and neon. Obviously the calculated curves in Fig. 6 reflect this difference in the ionization cross sections, while the experiment certainly does not. Complementary and consistent evidence of the role of the core dependent cross sections is clearly observed for the PES and HHG spectra both in the experiments and calculations.

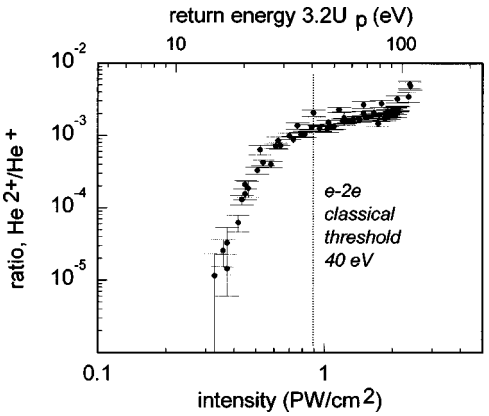

FIG. 7. The intensity-dependent ratio of nonsequential double-to-single ionization for helium at 0.39 μm. The upper abscissa scale gives the maximum return energy at this wavelength, and the dotted line marks the classical threshold.

A final piece of evidence that contradicts the predictions of the inelastic rescattering model for NS ionization is shown in Fig. 7. The plot shows the ratio of $He^{2+}(NS)/He^{+}$ as a function of intensity for 0.39-μm excitation. The shorter wavelength reduces the ponderomotive energy by a factor of 4, since it scales as ω^{-2}, which consequently decreases the return energy by the same factor. We note that this saturates before it becomes pure tunneling. The dotted line shows the intensity below which the return energy can no longer excite the core electron, that is $3.2U_p < 40$ eV, the excitation energy of the first excited state of helium. Again, all the nonsequential production is occurring below this threshold with a value (0.0013), which is not much different from the 0.78-μm result at saturation. These measurements reaffirm that inelastic rescattering cannot be the dominant mechanism for strong-field double ionization.

Although exact two-electron numerical solutions for multiphoton ionization of helium in intense pulsed laser fields have been obtained for short (extreme ultraviolet) wavelengths [38], these are far from the tunneling regime and not relevant to the NS ionization problem considered here. There have been, however, a number of model calculations for our experimental parameters that have produced much larger double-ionization yields than those we obtained with our model. One result by Becker and Faisal [39,40] using a quantum, two-electron perturbation expansion to calculate the *S*-matrix element for double ejection, leads to the conclusion that the fundamental mechanism is neither shake-off nor rescattering, but due to first one electron interacting with the field to absorb *virtually* a large number of photons, which is followed by the electron-electron correlation mediating the sharing of the energy until both escape together from the binding force of the nucleus. Using this approach, very impressive agreement with the linearly polarized, 780-nm data of Walker *et al.* [13] was obtained. Results for the strong ellipticity dependence of the NS yields or for other wavelengths have not been presented. We hope the data shown here will encourage further applications of this *S*-matrix formalism to validate the approach. Other model studies which explicitly test the efficacy of rescattering to induce NS ion-

ization also have replicated the existing 780-nm, linear polarization, data. We will briefly describe these other rescattering model calculations and try to explain what we believe are the sources of the differences from our results.

Using a semiclassical model for helium it was established that the oscillating laser field that tunnel ionizes the first electron has negligible effect on the collision-induced transition probabilities of the more tightly bound ion core states [37]. This means that using field-free cross sections in model rescattering calculations for the intensities that ionize the first electron will give reasonably accurate results. Recently there has been a similar, but more elaborate calculation of helium double ionization by Watson *et al.* [41], where both electrons were treated quantum mechanically. In this calculation the time evolution of the first ''outer'' electron is obtained by solving the SAE equation. The second ''inner'' electron begins in the same Hartree-Fock ground-state orbital of the neutral, and moves in the mean field of the charge distribution of the first electron, the nucleus, and the laser. A direct test of the rescattering mechanism is achieved by placing an absorbing boundary successively closer to the ion core, which eliminates the possibility of the TI wave packet returning to excite the inner electron. The results showed a large reduction in the double-ion yield, indicating that rescattering was the dominant mechanism for removing the second electron. The study found that the double ionization yield due to rescattering was even larger than that obtained in our experiments. Again, energy transfer from the first to the second electron is assumed not to alter the evolution of the first electron, which means that the inelastic probabilities near threshold may be too large. A more serious error is introduced by the mean-field approximation. During each half-cycle a TI wave packet is created which collides with the inner electron during the following cycle. However, through the mean-field interaction, the unexcited part of the outer electron-density distribution screens the nuclear attraction ''felt'' by the inner electron, reducing the effective ionization potential of the inner electron to 25 eV rather than the $\approx$54 eV of the real ion core. Similarly, the excitation threshold will be about 20 eV instead of 40 eV. Only as the ground-state density of the outer electron is depleted by ionization will the binding energy of the inner electron gradually approach the correct value. This must lead to a double-ionization rate which is much too large, especially at lower intensities. This is evident in Fig. 2 of Ref. [41], where the model's intensity threshold for NS ionization is significantly below that found in the experiment.

A second important rescattering calculation in Ref. [25] treated both electrons classically. Initially, the first electron appears on the outer edge of the suppressed potential barrier with zero velocity along the polarization axis and a distribution of velocities in the perpendicular direction. The width of the transverse velocity distribution is inversely proportional the instantaneous dc tunneling rate. The time evolution of this electron is followed for five cycles with the laser intensity fixed, then an additional 2.5 cycles during which the field is smoothly turned off. The state of the bound (inner) electron is given by a trajectory initially at rest at the origin of the coordinate system (the nucleus). This initial condition confines the motion of both electrons to the plane defined by the polarization axis and the direction of the initial transverse momentum. If the bound electron had an arbitrary, small displacement from the origin, the dynamics would be three dimensional (3D), and the equations of motion would be more complicated than those presented in their paper. It is not clear whether this unnecessary restriction affects the applicability of the results to the complete dynamics of the real system, but in calculating the cross sections, the probabilities appear to have been correctly weighted according to the azimuthal symmetry of the 3D atom. The main conclusion of this study was that although there is a small probability for impact ionization of the bound electron during the first return of the free electron, inclusion of additional returns can significantly enhance the efficiency of double ionization by trajectories with low drift velocities. This leads to an overall factor of 30 increase in the total NS yield relative to that obtained by considering only the first return. The authors of Ref. [25] attributed this enhancement to the refocusing of the trajectories by the Coulomb field, so that later returns produce much higher charge density near the nucleus. They concluded that this refocusing overwhelms the transverse expansion of the TI wave packet while it propagates (most of the time) in the region beyond the effective range of the ion core potential.

We can easily test the importance of refocusing for a real, quantum TI wave packet using the SAE approximation to calculate the strength of the generated high harmonics as a function of time after the wave packet is created. Since the harmonics are produced by transitions back to the ground state, this is an ideal probe of the density distribution of rescattering electrons near the nucleus. For helium, only the $l=1$ partial wave can contribute to this emission. We use a constant intensity pulse to produce a TI wave packet during the first half cycle. At this point, the time-dependent wave function is orthogonalized to the ground state, and the subsequent evolution represents only that of the excited-state component of the total wave function. As this TI wave packet is driven back and forth across the ion core, we can Fourier transform (FT) the dipole matrix element between the wave packet and the ground state. This approximate dipole has been shown to give very accurate harmonic emission strengths [42]. We can consider the spectra generated by different ''returns'' by restricting the time interval in the FT. We find that the emission rate during the first return is at least a factor of 10 stronger than that from the next two cycles, with later returns falling by more orders of magnitude. We must conclude that the Coulomb focusing is not sufficient to explain the substantial enhancement the authors of Ref. [25] found in their trajectory calculations. A more likely explanation for their result is that when the TI electron first returns, it can transfer a small amount of energy to the bound electron, becoming trapped in a low-lying ''doubly excited'' state. These states, which cannot exist in the quantum system, are allowed classically because the density of states is continuous. The TI electrons which are most important for the inelastic collisions (and the harmonic generation) are those with small drift energies. These are very likely to be captured, requiring more collisions before they can reescape. This will produce a very large enhancement of the NS ionization yield that would be completely absent in the real quantum system.

At this time, with perhaps the exception of the *S*-matrix

results, there has been no convincing theoretical demonstration of any explicit mechanism for the observed NS ionization. In the work of Becker and Faisal [39,40], the nature of the ''correlation'' which causes the transitions is still difficult to envision. Insight into the *S*-matrix method can be realized by application to the shorter wavelength results presented here, and to an investigation of the known ellipticity dependences. We believe progress in solving this problem conclusively will await more ambitious two-electron time-dependent calculations which can be analyzed to uncover the details of the double-emission dynamics.

V. CONCLUSIONS

This study exemplifies how over the past decade our perspective of the single electron dynamics has matured to a level of precise comparison between theory and experiment, aided by classical intuition. The same kHz laser technology, which facilitated an understanding of single-electron excitation, also provides additional evidence and raises some ''old'' questions regarding strong-field two-electron ionization.

The above discussion of the electron emission studies illustrates two salient features of the current investigation. First, the experimental PES behave in a manner consistent with our intuitive picture of a field-driven wave packet elastically recolliding with the atomic core. Second, the quality of this interpretation substantiates that the regime of ionization achieved in the current experiment is tunneling. The excellent agreement between the complete semiclassical rescattering model calculations and measurements for the electrons makes the disagreement with the NS ionization yields all the more compelling. There is clearly a real need for more realistic two-electron calculations which can exactly treat the correlated dynamics in order to establish the mechanism for double ionization firmly. Further experimental studies in the tunneling regime could also provide some insight into the underlying dynamics. The kHz laser technology provides an efficient tool to utilize coincidence measurement techniques, while investigations at longer wavelengths could broadening investigations into different atomic systems.

ACKNOWLEDGMENTS

This research was carried out in part at Brookhaven National Laboratory under Contract No. DE-AC02-98CH10886 with the U.S. Department of Energy, supported by its Division of Chemical Sciences, Office of Basic Energy Sciences, and in part under the auspices of the U.S. Department of Energy at the Lawrence Livermore National Laboratory under Contract No. W-7405-ENG-48. L.F.D. and P.A. acknowledge travel support from NATO under Contract No. SA.5-2-05(RG910678).

[1] For some recent advances in high-field applications, see *Applications of High Fields and Short Wavelength Sources*, edited by L. F. DiMauro, A. L'Huillier, and M. Murnane (Plenum, New York, 1998).
[2] For a review, see L. F. DiMauro and P. Agostini, in *Advances in Atomic, Molecular, and Optical Physics 35*, edited by B. Bederson and H. Walther (Academic, San Diego, 1995).
[3] M. Saeed, L. F. DiMauro, and S. Tornegard, Laser Focus World **27**, 57 (1991).
[4] For a review of time-dependent methods, see K. C. Kulander, K. J. Schafer, and J. L. Krause, in *Atoms in Intense Radiation Fields*, edited by M. Gavrila (Academic, New York, 1992).
[5] K. J. Schafer, B. Yang, L. F. DiMauro, and K. C. Kulander, Phys. Rev. Lett. **70**, 1599 (1993).
[6] P. B. Corkum, Phys. Rev. Lett. **71**, 1994 (1993).
[7] L. V. Keldysh, Zh. Eksp. Teor. Fiz. **47**, 1945 (1964) [Sov. Phys. JETP **20**, 1307 (1965)].
[8] K. C. Kulander and K. J. Schafer, in *Multiphoton Processes*, edited by D. K. Evans and S. L. Chin (World Scientific, Singapore, 1993), p. 391.
[9] P. B. Corkum, N. H. Burnett, and F. Brunel, Phys. Rev. Lett. **62**, 1259 (1989).
[10] S. Augst, D. D. Meyerhofer, D. Strickland, and S. L. Chin, J. Opt. Soc. Am. B **8**, 858 (1991).
[11] T. Auguste, P. Monot, L. A. Lompre, G. Mainfray, and C. Manus, J. Phys. B **25**, 4181 (1992).
[12] U. Mohideen, M. H. Sher, H. W. K. Tom, G. D. Aumiller, O. R. Wood II, R. R. Freeman, J. Bokor, and P. H. Bucksbaum, Phys. Rev. Lett. **71**, 509 (1993).
[13] B. Walker, B. Sheehy, L. F. DiMauro, P. Agostini, K. J. Schafer, and K. C. Kulander, Phys. Rev. Lett. **73**, 1227 (1994).
[14] B. Walker, B. Sheehy, K. C. Kulander, and L. F. DiMauro, Phys. Rev. Lett. **77**, 5031 (1996).
[15] G. G. Paulus, W. Becker, W. Nicklich, and H. Walther, J. Phys. B **27**, L1 (1994).
[16] M. Lewenstein, K. C. Kulander, K. J. Schafer, and P. H. Bucksbaum, Phys. Rev. A **51**, 1495 (1995).
[17] W. Becker, A. Lohr, and M. Kleber, J. Phys. B **27**, L325 (1994).
[18] L. I. Schiff, *Quantum Mechanics*, 3rd ed. (McGraw-Hill, New York, 1968).
[19] B. Gottlieb, A. Lohr, W. Becker, and M. Kleber, Phys. Rev. A **54**, R1022 (1996).
[20] G. G. Paulus, F. Zacher, H. Walther, A. Lohr, W. Becker, and M. Kleber, Phys. Rev. Lett. **80**, 484 (1998).
[21] M. V. Ammosov, N. B. Delone, and V. P. Krainov, Zh. Eksp. Teor. Fiz. **91**, 2008 (1986) [Sov. Phys. JETP **64**, 1191 (1986)].
[22] Baorui Yang, K. J. Schafer, B. Walker, K. C. Kulander, P. Agostini, and L. F. DiMauro, Phys. Rev. Lett. **71**, 3770 (1993).
[23] A. L'Huillier and Ph. Balcou, Phys. Rev. Lett. **70**, 774 (1993).
[24] H. R. Reiss, Phys. Rev. A **54**, R1765 (1996).
[25] T. Brabec, M. V. Ivanov, and P. B. Corkum, Phys. Rev. A **54**, R2551 (1996).
[26] J. H. McGuire, N. Berrah, R. J. Bartlett, J. A. R. Samson, J. A. Tanis, C. L. Cocke, and A. S. Schlachter, J. Phys. B **28**, 913 (1995).
[27] P. Lambropoulos, Phys. Rev. Lett. **55**, 2141 (1985).
[28] B. Walker, E. Mevel, B. Yang, P. Berger, J. P. Chambaret, A. Antonetti, L. F. DiMauro, and P. A. Agostini, Phys. Rev. A **48**, R894 (1993).

[29] D. Charalambidis, P. Lambropoulos, H. Schröder, O. Faucher, H. Xu, M. Wagner, and C. Fotakis, Phys. Rev. A **50**, R2822 (1994).
[30] L. A. Lompre and G. Mainfray, in *Multiphoton Processes*, edited by P. Lambropoulos and S. J. Smith (Springer-Verlag, Berlin, 1984), p. 23.
[31] D. L. Fittinghoff, P. B. Bolton, B. Chang, and K. C. Kulander, Phys. Rev. Lett. **69**, 2642 (1992).
[32] P. Dietrich, N. H. Burnett, M. V. Ivanov, and P. B. Corkum, Phys. Rev. A **50**, R3585 (1994).
[33] S. Augst, A. Tablebpour, S. L. Chin, Y. Beaudoin, and M. Chaker, Phys. Rev. A **52**, R917 (1995).
[34] D. L. Fittinghoff, P. B. Bolton, B. Chang, and K. C. Kulander, Phys. Rev. A **49**, 2174 (1994).
[35] K. Kondo, A. Sagisaka, T. Tamida, Y. Nabekawa, and S. Watanabe, Phys. Rev. A **48**, R2531 (1993).
[36] W. Lotz, Z. Phys. **216**, 241 (1968).
[37] K. C. Kulander, J. Cooper, and K. J. Schafer, Phys. Rev. A **51**, 561 (1995).
[38] P. Lambropoulos, P. Maragakis and J. Zhang, Phys. Rep. **305**, 203 (1998), and references therein.
[39] A. Becker and F. H. M. Faisal, J. Phys. B **29**, L197 (1996).
[40] F. H. M. Faisal and A. Becker, Laser Phys. **7**, 684 (1997).
[41] J. B. Watson, A. Sanpera, D. G. Lappas, P. L. Knight, and K. Burnett, Phys. Rev. Lett. **78**, 1884 (1997).
[42] K. J. Schafer, J. L. Krause, and K. C. Kulander, Int. J. Nonlinear Opt. Phys. **1**, 245 (1992).